Formation of Poly(ethylene glycol)-Poly(ε-caprolactone) Nanoparticles via Nanoprecipitation

Jae Sung Lee, Su Jong Hwang, and Doo Sung Lee*

Department of Polymer Science & Engineering, Sungkyunkwan University, Gyeonggi 440-746, Korea

Sung Chul Kim

Department of Chemical and Biomolecular Engineering, Korea Advanced Institute of Science and Technology, Daejeon 305-701, Korea

Duk Joon Kim

Department of Chemical Engineering, Sungkyunkwan University, Gyeonggi 440-746, Korea

Abstract: Size control of therapeutic carriers in drug delivery systems has become important due to its relevance to biodistribution in the human body and therapeutic efficacy. To understand the dependence of particle size on the formation condition during nanoprecipitation method, we prepared nanoparticles from biodegradable, amphiphilic block copolymers and investigated the particle size and structure of the resultant nanoparticles according to various process parameters. We synthesized monomethoxy poly(ethylene glycol)-poly(ε-caprolactone) block copolymer, MPEG-PCL, with different MPEG/PCL ratios via ring opening polymerization initiated from the hydroxyl end group of MPEG. Using various formulations with systematic change of the block ratio of MPEG and PCL, solvent choice, and concentration of organic phase, MPEG-PCL nanoparticles were prepared through nanoprecipitation technique. The results indicated that (i) the nanoparticles have a dual structure with an MPEG shell and a PCL core, originating from self-assembly of MPEG-PCL copolymer in aqueous condition, and (ii) the size of nanoparticles is dependent upon two sequential processes: diffusion between the organic and aqueous phases and solidification of the polymer.

Keywords: nanoparticle, drug delivery, nanoprecipitation, poly(ε-caprolactone).

Introduction

Nontoxic, biodegradable polyesters, for example, polylactide (PLA), poly(lactide-*co*-glycolide) (PLGA) and poly(ε-caprolactone) (PCL), have been focused as one of the most versatile materials in bio-related fields, for example, orthopedic implant,[1-4] scaffold for tissue regeneration,[5-11] and delivery system of therapeutic substances such as drugs,[12-18] protein,[19,20] and oligonucleotide like RNA and DNA.[21-23] A great deal of different strategies for modification of these polymeric materials has been also intensively reported with the aim of fine-tuning of physicochemical properties on demand for practical applications by means of (i) chemically conjugation through copolymerization with poly(ethylene glycol) (PEG)[24-27] or biologically benign moieties,[28-31] and (ii) surface modification via surface coating,[32-34]

blend,[35,36] and plasma treatment.[37] Those modifications make it possible to readily tailor the hydrophilicity,[32,35] specific interaction,[32-37] and other desired functions.[24,26,27]

Specifically, block copolymer of polyester with featured components facilitates colloidal drug delivery carrier to be highly efficient in sustained release on specific target site. Colloidal carriers of polyester copolymer incorporated with PEG exhibit superior biodistribution by prolonged circulation in blood system because the mobile PEG brush serves as a protective shield around the particulate, significantly suppressing undesired adsorption of blood proteins onto therapeutic particulate.[38-41] Another way to realize long circulating particles is to adjust the particle size (~200 nm) enough to avoid phagocytosis by protein adsorption.[42-44] This is the reason why nanoparticles as drug delivery vehicle have been of great concern as a promising alternative to achieve so-called "missile delivery" in controlled manner. There have been proposed a variety of fabrication tech-

*Corresponding Author. E-mail: dslee@skku.edu

niques for nanoparticles, e.g., emulsion,[45] double-emulsion,[46] phase separation/dialysis,[47] and nanoprecipitation method.[48,49] Depending on selection of production method, one would be able to control the structure and physicochemical property of particulate, cargo loading, and subsequent cargo release. In particular, nanoprecipitation method we will deal here offers a simple and easy process; nano-sized particles can be produced by just dropping polymer-containing organic phase into nonsolvent bath. This technique is mainly based on the solidification of polymer caused by inter-diffusion between organic phase and surrounding nonsolvent medium, and thus good miscibility of solvent and nonsolvent should be fulfilled.

The aim of the present study is to examine the relationship of nanoparticle size and the process parameters of nanoprecipitation method. To this end, we synthesized monomethoxy poly(ethlylene glycol)-poly(ε-caprolactone) block copolymer as a model material and investigated the size of nanoparticles according to concentration of organic phase, choice of solvent and block ratio of each block in monomethoxy poly(ethylene glycol)-poly(ε-caprolactone) block copolymer. General understanding of the effect of fabrication conditions on particle size would provide a serviceable tool to decide the formulation to achieve desired particle size.

Experimental

Materials. Monomethoxy poly(ethylene glycol) (MPEG, M_n of 5,000 g/mol), ε-caprolactone (CL), and poly(ε-caprolactone) (PCL, M_n of 1,000) were purchased from Aldrich, USA. Stannous 2-ethyl hexanoate (Sn(Oct)$_2$), dichloromethane, CDCl$_3$ and D$_2$O were also received from Aldrich, USA. Diethyl ether, methanol, tetrahydrofuran (THF), acetone, acetonitrile were supplied from Samchun Pure Chemical, Korea. All chemicals and reagents were used as received without further purification unless stated otherwise.

Synthesis of Monomethoxy Poly(ethylene glycol)-Poly(ε-caprolactone). The synthesis of monomethoxy poly(ethylene glycol)-poly(ε-caprolactone) block copolymer (MPEG-PCL) was done through a ring-opening copolymerization, using MPEG and Sn(Oct)$_2$ as an initiator and a catalyst respectively. MPEG and Sn(Oct)$_2$ (0.5 wt%) were placed in a two-neck round-bottom flask and dried for 3 h at 110 °C under reduced pressure. After cooling to 50 °C, CL monomer was added into the flask under nitrogen atmosphere and then the reactant mixture was dried again in vacuum for 1 h to remove the moisture thoroughly. The temperature was raised slowly to 150 °C to trigger the ring-opening copolymerization, and kept for 24 h. After reaction, the product mixture was cooled down to room temperature, dissolved in dichloromethane, and precipitated in excess methanol. The precipitated MPEG-PCL block copolymer was filtrated to remove remaining reactants, which was followed by wash-

ing with diethyl ether. The obtained MPEG-PCL was vacuum-dried at 40 °C for 3 days.

Preparation of Nanoparticles via Nanoprecipitation Method. First, MPEG-PCL block copolymer was dissolved in the 10 mL of organic solvent at predetermined concentrations. Three different organic solvents (i.e., acetone, acetonitrile and THF) were adopted to vary the solvent quality. The polymer solution was added dropwise into the deionized water (100 mL) under magnetic stirring and kept for 20 min. Then the organic solvent was evaporated under reduced pressure using rotary evaporator, resulting in the nanoparticles in aqueous solution.

^{1}H Nuclear Magnetic Resonance (^{1}H NMR) Spectroscopy. ^{1}H NMR spectrum of synthesized block copolymer in CDCl$_3$ was measured on a Varian-Unity Inova 500NB to determine the molecular weight and copolymer composition. As the number-average molecular weight of MPEG is known as 5,000 g/mol, molecular weight of poly(ε-caprolactone) block and composition of each block can be calculated by comparison of the typical proton peak integration of MPEG and CL in ^{1}H NMR spectra. Also, the structure of nanoparticles was verified through comparison of ^{1}H NMR spectra of MPEG-PCL nanoparticles in CDCl$_3$ and D$_2$O.

Characterization of Nanoparticle. The size of resultant nanoparticles was determined by dynamic light scattering (DLS) using Malvern PCS100 goniometer and Brookhaven BI-9000AT digital autocorrelator. Nanoparticles were dispersed in deionized water at a concentration of 1 mg/mL and passed through a 1.20 μm syringe filter prior to measurement. The measurements were carried out at a scattering angle of 90 °C. The CONTIN algorithms were used in the Laplace inversion of the autocorrelation function to obtain micelle size. The mean diameter was evaluated from the Stokes-Einstein equation. Measurement for each sample was performed in triplicate. Surface charge of nanoparticles was characterized in terms of zeta potential using zeta potential analyzer, (Zetasizer 3000, Malvern instruments). Before measurement, the particle suspension was diluted with deionized water to 1 mg/mL. The values were recorded as the average of five measurements. The morphology of nanopartilcles was observed by field emission scanning electron microscopy (FE-SEM, JSM-6700F, JEOL). The particle-suspended aqueous solution was dropped on the mount, and the water was allowed to evaporate slowly at room temperature. Prior to observation, the sample was coated with platinum.

Results and Discussion

Synthesis of MPEG-PCL Diblock Copolymer. To control the hydrophilicity of block copolymer, block length of hydrophobic PCL was systematically modulated with constant hydrophilic MPEG block length by changing the feed ratio of CL and MPEG. The chemical structure of MPEG-
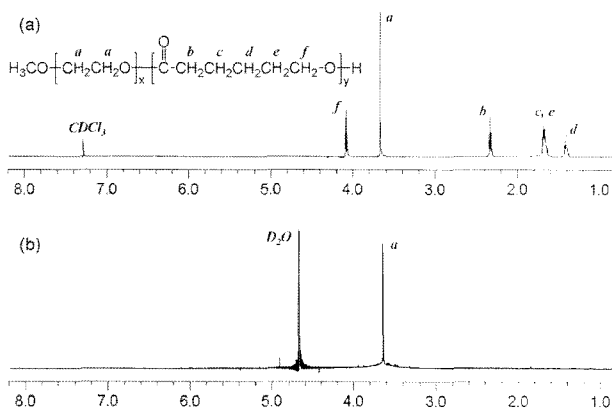
Figure 1. Typical ^{1}H NMR spectra of (a) PECL block copolymer or PECL nanoparticles in CDCl$_3$ and (b) PECL nanoparticles in D$_2$O.

**Table I. Ratio of MPEG and PCL for Synthesized MPEG-PCL Block Copolymer**

Notation	Copolymer Weight Ratio ($M_{n,MPEG}:M_{n,PCL}$)	
	Theoretical (by feed ratio)	Experimental (by ^{1}H NMR)
PECL-100	5,000 : 5,000	5,000 : 5,100
PECL-200	5,000 : 10,000	5,000 : 9,800
PECL-360	5,000 : 15,000	5,000 : 18,000

PCL copolymer and the ratio of MPEG and PCL were verified with ^{1}H NMR in CDCl$_3$. Figure 1(a) displays a typical ^{1}H NMR spectrum of MPEG-PCL block copolymer. The number of repeating units of PCL block, y, was determined from the following equation, based on the ratio of characteristic peaks from each block.

$$\frac{2y}{4x} = \frac{I_c}{I_b}$$

where x, the repeating number of oxymethylene, is known to be 113 from the molecular weight of MPEG (M_n of 5,000), and I_b and I_c are the integrated area of corresponding peak for a and b, respectively. From the calculated y value, we were able to estimate the molecular characteristics of synthesized MPEG-PCL block copolymer (see Table I). For the sake of convenience, MPEG-PCL block copolymer will be hereafter represented as a notation of PECL or PECL-xxx, where xxx denotes the percentage ratio of molecular weight of PCL block to that of MPEG counterpart, which was determined from NMR analysis described above. As can be seen in Table I, three PECL block copolymers with different MPEG/PCL ratio were prepared, and GPC trace for the synthesized polymers displayed a unimodal and narrow peak (not shown here). These results confirmed that the PECL block copolymer with narrow molecular weight distribution was successfully prepared.
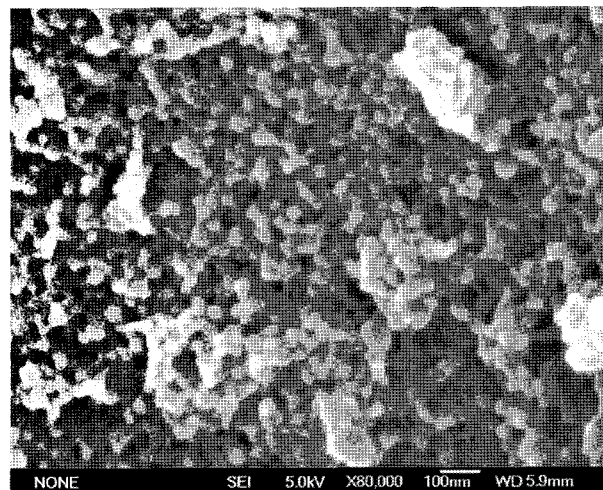

Figure 2. FE-SEM micrograph of nanoparticles made from 10 mg/mL PECL-100 solution in THF. Scale bar indicates 100 nm.

Table II. Mean Diameter of Nanoparticles Prepared by Nanoprecipitation Method with Various Processing Condition

Solvent	Concentration of Organic Phase	Mean Diameter (nm)		
		PECL-100	PECL-200	PECL-360
Acetone	10 mg/mL	53.9 ± 3.9	66.3 ± 4.6	78.0 ± 2.6
	20 mg/mL	58.3 ± 8.1	68.0 ± 2.6	85.8 ± 4.0
	30 mg/mL	60.8 ± 3.2	74.0 ± 3.6	97.8 ± 5.8
Acetonitrile	10 mg/mL	60.7 ± 1.5	69.5 ± 5.9	83.1 ± 3.8
	20 mg/mL	64.8 ± 6.5	67.0 ± 2.7	103.7 ± 4.7
	30 mg/mL	71.3 ± 7.4	76.0 ± 4.9	114.8 ± 5.9
THF	10 mg/mL	60.2 ± 4.6	77.4 ± 4.6	123.7 ± 9.1
	20 mg/mL	66.5 ± 2.7	102.0 ± 8.8	150.7 ± 9.0
	30 mg/mL	72.6 ± 6.4	130.0 ± 10.4	152.3 ± 7.5

Particle Size and Surface Charge. During nanoprecipitation technique, the particles are formed by the solidification of polymer as a result of diffusional exchange of solvent and nonsolvent. We employed acetone, acetonitrile, and THF as an organic solvent, and water as a nonsolvent medium. Since the organic solvents used here are all miscible to water, the solvent in organic phase migrates spontaneously toward water phase once the polymer solution in organic solvent is introduced into water. Sudden change of the solvent composition around the polymer molecules finally induces solidification of polymer (i.e., precipitation by crystallization or vitrification) and subsequently nanoparticle formation. During this process, the diffusion rate is expected to be governed largely by the polymer-solvent, polymer-nonsolvent and solvent-nonsolvent interaction as well as viscosity of polymer solution. We investigated the effect of these factors on the nanoparticle size qualitatively by changing (i) composition of MPEG and PCL in PECL

74
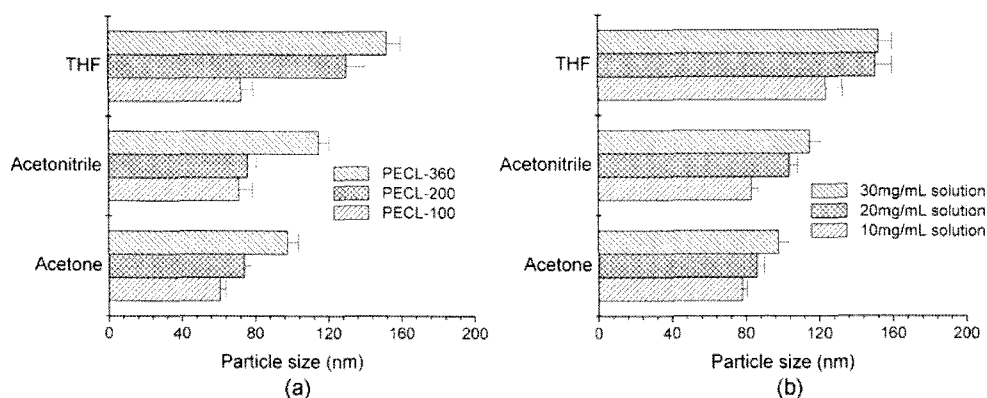
Figure 3. Particle size of (a) PECL nanoparticles made from 30 mg/mL solution and (b) PECL-360 nanoparticles.

block copolymer, (ii) selection of solvent, and (iii) concentration of polymer solution.

Table II summarized the sizes of PECL nanoparticles produced through various formulation conditions in nanoprecipitation technique. Figure 2 shows SEM picture of PECL-200 nanoparticles prepared from 10 mg/mL THF solution. The size of all nanoparticles covered the range of 50 and 150 nm regardless of process formulation. This advantageous nano-scale dimension enables the therapeutic colloidal objects to avoid the cellular uptake by mononuclear phagocyte system (MPS), which has imposed a major limitation on the targeted local drug delivery. As for the structure of PECL nanoparticles, comparison of Figure 1(a) and (b) allowed to estimate chain distribution in obtained nanoparticles. ^{1}H NMR spectrum of PECL particles recorded in CDCl$_3$ was exactly the same as that obtained from PECL solution in CDCl$_3$, because both MPEG and PCL block would be fully solubilized into CDCl$_3$. In contrast, proton NMR of PECL particles in D$_2$O displayed only a typical peak that corresponds to the protons of MPEG (Figure 1(b)), indicating that the MPEG moieties of PECL block are exposed to the outer surface of PECL nanoparticles. The difference in NMR spectrum of PECL particle in CDCl$_3$ and D$_2$O elucidated that nanoparticles made from amphiphilic PECL via nanoprecipitation technique has a core-shell structure of hydrophobic PCL core and hydrophilic MPEG shell. This could be confirmed from the value of zeta potential, which will be discussed later.

We investigated the influence of a couple of process parameters of nanoprecipitation technique on the final PECL nanoparticles. Firstly, the effect of the molecular characteristic of PECL block copolymer was examined in terms of the ratio of PCL and MPEG block. The hydrophilicity of PECL block copolymer is determined by the ratio of hydrophilic MPEG moiety and hydrophobic PCL segment; longer PCL chain with a given MPEG block would impose stronger hydrophobicity of entire molecule, and induce a growing tendency for the block copolymer to self-aggregate upon water contact. Considering this aspect of PECL mole-

cule, the particle size variation according to the block ratio of PCL to MPEG was easily understood. As shown in Figure 3(a) and Table II, at a given solvent and a given polymer concentration, the particle size increased when nanoparticles were prepared from more hydrophobic PECL with longer PCL block. As soon as PECL solution in organic solvent was introduced into water during nanoprecipitation process, it diffused and split into smaller domains in water medium, and finally precipitated into nanoparticles. Although diffusion and precipitation occurred almost simultaneously, the final dimension of resultant nanoparticles was determined by amount of polymer molecules in the vicinity available for aggregation when the solidification completed. Upon the increment of PCL block with a fixed length of MPEG counterpart, PCL blocks in more hydrophobic PECL molecules preferred to assemble together by hydrophobic interaction between PCL block rather than disperse in aqueous solution, which made more PECL molecules take part in the solidification process leading to formation of bigger particles.

As for how the concentration of polymer solution would affect the particle size, we found out that more concentrated solution produced bigger particulates as expected (Figure 3(b)). As the polymer composition of organic phase was increased from 10 to 30 mg/mL, the obtained nanoparticles became bigger by 10 to 50 nm depending on polymer-solvent pair. Solution composition brought about the change of viscosity of organic phase, and thus affected the diffusion rate between organic phase and aqueous coagulation phase; higher concentration in organic phase induced more viscous media and slow diffusion, making it difficult for organic phase to disperse into aqueous phase. Consequently, the organic domains were solidified before they were dispersed into smaller ones, and bigger particles were formed.

To see the effect of solvent choice on particle size, we employed three different solvents for this study. As can be seen in Table II and Figure 3, we were able to control the PECL particle size with solvent selection. The size of nanoparticles decreased in order of THF, acetonitrile, and ace-

Table III. Hansen's and Hoy's Solubility Parameters and Calculated Interaction Parameters

|	$\delta_{dispersion}$ (MP$^{1/2}$)		δ_{polar} (MP$^{1/2}$)		$\delta_{hydrogen\ bonding}$ (MP$^{1/2}$)		$\Delta\delta_{solvent-water}$ (MP$^{1/2}$)		$\chi_{solvent-water}$	
	Hansen	Hoy	Hansen	Hoy	Hansen	Hoy	Hansen	Hoy	Hansen	Hoy
Acetone	15.5	13.0	10.4	9.8	7.0	11.0	35.7	32.1	23.2	23.9
Acetonitrile	15.3	10.3	18.0	11.1	6.1	19.6	36.3	23.9	11.6	11.4
THF	16.8	13.3	5.7	11.0	8.0	6.6	35.8	35.8	26.5	28.7
Water	15.5	12.2	16.0	22.7	42.3	40.4	-	-	-	-

$$\Delta\delta_{solvent-water} = [\delta_{dispersion,solvent}-\delta_{dispersion,water}]^2 + (\delta_{polar,solvent}-\delta_{polar,water})^2 + (\delta_{hydrogen\ bonding,solvent}-\delta_{hydrogen\ bonding,water})^2]^{1/2}.$$

$$\chi_{solvent-water} = \frac{V_{solvent}}{RT}(\delta_{solvent}-\delta_{water})^2.$$

tone. Solvent change on nanoprecipitation process would induce complicated alternation between solvent-polymer interaction, solvent-nonsolvent interaction, and diffusion process. Doelker *et al.* have revealed the relationship between solvent-water interaction parameter and nanoparticle size.[49] The nanoparticle size made by nanoprecipitation technique was decreased as the solvent of higher affinity with water was employed as organic phase, because promoted solvent diffusion and polymer chain partitioning in aqueous phase. They also reported the interaction parameter of water-solvent was proportional to the particle size. Cheng and his coworkers showed the size of PLGA-PEG nanoparticles was inversely proportional to the solvent-water affinity.[50] However, we were not able to see any correlation between solvent-water miscibility and particle size in our system. The interaction parameter between solvent and water, calculated from Hoy's method[51] and Hansen's method,[52] increases in order of acetonitrile, acetone, and THF, which indicates acetonitrile has best affinity to water and THF is the worst among them. Table III shows the calculated interaction parameters and equations for calculation. The solvent-water interaction parameter did not have any relation with nano-

particle size, which increases in order of acetone, acetonitrile, and THF. As for present study, simple relationship between solvent/water miscibility could not explain the tendency of nanoparticle size toward solvent. The other factors caused by solvent change, such as solvent-polymer interaction, viscosity of the organic phase, and any possible interaction with other components should be considered for more reliable prediction on particle size.

Figure 4 shows typical results on the size distribution of nanoparticles. The size distribution became broad at the conditions where the smaller particles were obtained (i.e., lower viscosity, better hydrophilicity and THF solvent). This could be interpreted with a competitive process between propagation of organic phase into surrounding medium and solidification of polymer. It is likely that the solidification was done in the middle of propagation of organic phase before reaching equilibrium size of organic phase in aqueous medium. If the propagation of organic phase made progress to more extent at the moment of solidification, the organic phase might randomly disperse and have broad size distribution. This is why the large size distribution was observed with smaller particles. In contrast, when the solidification
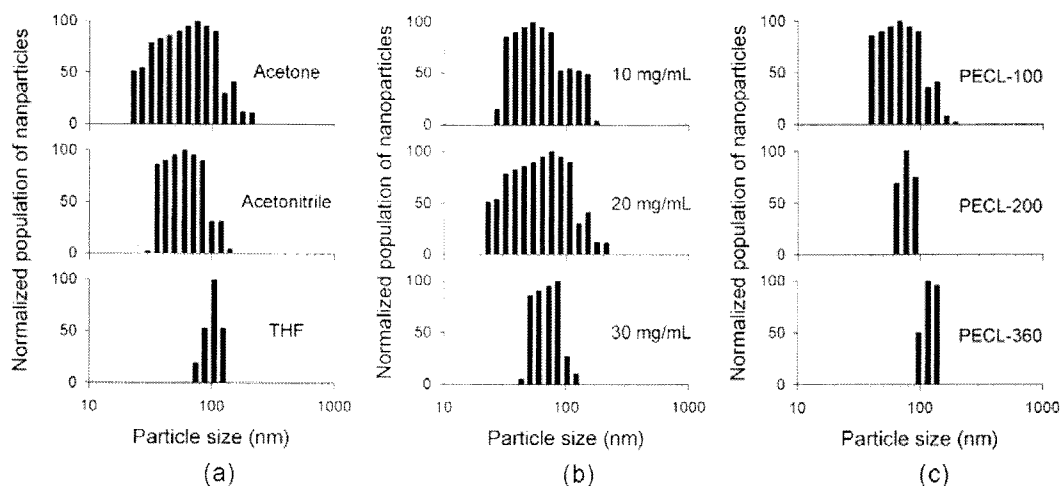
Figure 4. Size distribution of nanoparticles prepared by nanoprecipitation method; (a) 20 mg/mL PECL-200 solution, (b) PECL-200 solution in acetone, and (c) 10 mg/mL polymer solution in THF.

Table IV. Mean Diameter and Zeta Potential of PECL Nanoparticles Prepared from Various Conditions

Material	Polymer Solution		Mean Diameter (nm)	Zeta Potential (mV)
	Concentration	Solvent		
PCL	10 mg/mL	THF	924.3 ± 94.1	-49.3 ± 1.6
PECL-100			60.2 ± 4.6	-14.6 ± 4.0
PECL-200	10 mg/mL	THF	77.4 ± 4.6	-11.4 ± 4.3
PECL-360			123.7 ± 9.1	-9.1 ± 5.0
	10 mg/mL		77.4 ± 4.6	-11.4 ± 4.3
PECL-200	20 mg/mL	THF	102.0 ± 8.8	-2.2 ± 0.7
	30 mg/mL		130.8 ± 10.4	-2.4 ± 1.0
		Acetone	66.3 ± 4.6	-10.6 ± 4.1
PECL-200	10 mg/mL	Acetonitrile	69.5 ± 5.9	-11.2 ± 2.7
		THF	77.4 ± 4.6	-11.4 ± 4.3

occurred at the earlier stage of propagation process, the particle size would be relatively uniform but relatively bigger.

Table IV summarized the zeta potential result of PECL nanoparticles fabricated through various process parameters. The zeta potential values for PECL particles were ranging from -20 to 0 mV, whereas that of pure PCL particle (~900 nm) was around -50 mV. The decrease in the absolute value of zeta potential is attributed to the presence of MPEG moiety at the corona of the particle. The molecular conformation of PECL nanoparticles can be inferred from the weakened electrostatic negativity. The self-assembly of PECL molecules in aqueous condition during nanoprecipitation process induced a core-shell structure of hydrophobic PCL core and hydrophilic MPEG corona. Many researches has already demonstrated that PEG-shielded object shows reduced plasma protein adsorption and interaction with phagocytic cells, enabling efficient delivery through human blood stream without undesirable elimination by protective immune system. The subtle decrease in zeta potential with increasing PCL block can be properly explained from the fact that longer PCL portion arise stronger driving force for the aggregation of PCL moieties, helping facilitate the partitioning between MPEG outer corona and PCL inner core. Also, viscous organic solution allows relatively longer time for PECL macromolecules to arrange readily into favorable conformation, which would promote phase separation into hydrophobic aggregate and hydrophilic shell in aqueous condition.

Conclusions

Amphiphilic, biodegradable PECL diblock copolymers with various ratios of PCL to MPEG were synthesized by ring opening reaction, using MPEG as an initiator. The PECL nanoparticles were prepared via nanoprecipitation technique, and the relationship of resultant nanoparticles

and process parameters (such as solvent choice, concentration of polymer solution and ratio of MPEG and PCL block) was investigated in terms of particle size and zeta potential. The ^{1}H NMR study and zeta potential revealed that PECL nanoparticles have a beneficial core-shell structure, which is composed of protein-protective MPEG corona and biodegradable PCL core. According to DLS data, as higher concentration of organic phase or longer PCL block with a fixed MPEG block was employed, the resultant particle became bigger because of higher viscosity and in part, stronger hydrophobicity. This study showed the size of nanoparticles prepared via nanoprecipitation method could be readily tailored as desired by adjusting process variables.

References

(1) H. Pihlajamaki, O. Bostman, O. Tynninen, and O. Laitinen, *Bone*, **39**, 932 (2006).

(2) O. Laitinen, H. Pihlajamaki, A. Sukura, and O. Bostman, *J. Biomed. Mater. Res.*, **61**, 33 (2002).

(3) Q. Huang, D. W. Hutmacher, and E. H. Lee, *Tissue Eng.*, **8**, 469 (2002).

(4) R. C. Edwards, K. D. Kiely, and B. L. Eppley, *J. Oral Maxil. Surg.*, **59**, 19 (2001).

(5) H. Yoshimoto, Y. M. Shin, H. Terai, and J. P. Vacanti, *Biomaterials*, **24**, 2077 (2003).

(6) Y. Z. Zhang, Z. M. Huang, X. J. Xu, C. T. Lim, and S. Ramakrishna, *Chem. Mater.*, **16**, 3406 (2004).

(7) V. J. Chen, L. A. Smith, and P. X. Ma, *Biomaterials*, **27**, 3973 (2006).

(8) H. W. Ouyang, S. L. Toh, J. Goh, T. E. Tay, and K. Moe, *J. Biomed. Mater. Res. B*, **75B**, 264 (2005).

(9) W. J. Li, C. T. Laurencin, E. J. Caterson, R. S. Tuan, and F. K. Ko, *J. Biomed. Mater. Res.*, **60**, 613 (2002).

(10) Y. K. Luu, K. Kim, B. S. Hsiao, B. Chu, and M. Hadjiargyrou, *J. Control. Release*, **89**, 341 (2003).

(11) C. T. Lee, C. P. Huang, and Y. D. Lee, *Biomacromolecules*, **7**, 2200 (2006).

(12) R. T. Liggins and H. M. Burt, *Int. J. Pharm.*, **222**, 19 (2001).

(13) F. X. Hu, K. G. Neoh, and E. T. Kang, *Biomaterials*, **27**, 5725 (2006).

(14) H.Y. Lee, S. A. Yu, K. H. Jeong, and Y. J. Kim, *Macromol. Res.*, **15**, 547 (2007).

(15) T. Govender, S. Stolnik, M. C. Garnett, L. Illum, and S. S. Davis, *J. Control. Release*, **57**, 171 (1999).

(16) H. Zhang and S. Gao, *Int. J. Pharm.*, **329**, 122 (2007).

(17) X. B. Xiong, A. Mahmud, H. Uludag, and A. Lavasanifar, *Biomacromolecules*, **8**, 874 (2007).

(18) C. Allen, Y. S. Yu, D. Maysinger, and A. Eisenberg, *Bioconjugate Chem.*, **9**, 564 (1998).

(19) G. Z. Zhu, S. R. Mallery, and S. P. Schwendeman, *Nat. Biotechnol.*, **18**, 52 (2000).

(20) M. Lee, T. T. Chen, M. L. Iruela-Arispe, B. M. Wu, and J. C. Y. Dunn, *Biomaterials*, **28**, 1862 (2007).

(21) E. Walter, K. Moelling, J. Pavlovic, and H. P. Merkle, *J. Control. Release*, **61**, 361 (1999).

(22) H. Cohen, R. J. Levy, J. Gao, I. Fishbein, V. Kousaev, S. Sosnowski, S. Slomkowski, and G. Golomb, *Gene Ther.*, **7**, 1896 (2000).

(23) X. D. Yuan, L. Li, A. Rathinavelu, J. S. Hao, M. Narasimhan, M. He, V. Heitlage, L. Tam, S. Viqar, and M. Salehi, *J. Nanosci. Nanotechno.*, **6**, 2821 (2006).

(24) J. H. You, S. W. Choi, J. H. Kim, and Y. T. Kwak, *Macromol. Res.*, **16**, 609 (2008).

(25) S. R. Bhattarai, N. Bhattarai, H. K. Yi, P. H. Hwang, D. I. Cha, and H. Y. Kim, *Biomaterials*, **25**, 2595 (2004).

(26) S. J. Im, Y. M. Choi, E. Subramanyam, K. M. Huh, and K. Park, *Macromol. Res.*, **15**, 363 (2007).

(27) C. Choi, M. Jang, and J. Nah, *Macromol. Res.*, **15**, 623 (2007).

(28) C. Deng, H. Y. Tian, P. B. Zhang, J. Sun, X. S. Chen, and X. B. Jing, *Biomacromolecules*, **7**, 590 (2006).

(29) C. Park, M. Rhue, J. Lim, and C. Kim, *Macromol. Res.*, **15**, 39 (2007).

(30) S. C. Lee, C. Kim, I. C. Kwon, H. Chung, and S. Y. Jeong, *J. Control. Release*, **89**, 437 (2003).

(31) P. Ping, W. S. Wang, X. S. Chen, and X. B. Jing, *Biomacromolecules*, **6**, 587 (2005).

(32) J. S. Lee, S. H. Kim, Y. J. Kim, T. Akaike, and S. C. Kim, *Biomacromolecules*, **6**, 1906 (2005).

(33) Z. W. Ma, C. Y. Gao, Y. H. Gong, and J. C. Shen, *Biomaterials*, **26**, 1253 (2005).

(34) S. Barbault-Foucher, R. Gref, P. Russo, J. Guechot, and A. Bochot, *J. Control. Release*, **83**, 365 (2002).

(35) S. H. Oh, S. G. Kang, E. S. Kim, S. H. Cho, and J. H. Lee, *Biomaterials*, **24**, 4011 (2003).

(36) F. L. Mi, Y. M. Lin, Y. B. Wu, S. S. Shyu, and Y. H. Tsai, *Biomaterials*, **23**, 3257 (2002).

(37) S. Y. Kim, S. H. Cho, Y. M. Lee, and L. Y. Chu, *Macromol. Res.*, **15**, 646 (2007).

(38) J. C. Leroux, E. Allemann, F. DeJaeghere, E. Doelker, and R. Gurny, *J. Control. Release*, **39**, 339 (1996).

(39) R. Gref, Y. Minamitake, M. T. Peracchia, V. Trubetskoy, V. Torchilin, and R. Langer, *Science*, **263**, 1600 (1994).

(40) R. L. Juliano, *Adv. Drug Deliver. Rev.*, **2**, 31 (1988).

(41) V. P. Torchilin and V. S. Trubetskoy, *Adv. Drug Deliver. Rev.*, **16**, 141 (1995).

(42) S. M. Moghimi, A. C. Hunter, and J. C. Murray, *Pharmacol. Rev.*, **53**, 283 (2001).

(43) G. Storm, S. O. Belliot, T. Daemen, and D. D. Lasic, *Adv. Drug Deliver. Rev.*, **17**, 31 (1995).

(44) Z. Gatmaitan, L. Varticovski, L. Ling, R. Mikkelsen, A. M. Steffan, and I. M. Arias, *Am. J. Pathol.*, **148**, 2027 (1996).

(45) C. X. Song, V. Labhasetwar, H. Murphy, X. Qu, W. R. Humphrey, R. J. Shebuski, and R. J. Levy, *J. Control. Release*, **43**, 197 (1997).

(46) W. Lu, Y. Zhang, Y. Z. Tan, K. L. Hu, X. G. Jiang, and S. K. Fu, *J. Control. Release*, **107**, 428 (2005).

(47) W. S. Shim, J. S. Lee, and D. S. Lee, *Macromol. Res.*, **13**, 344 (2005).

(48) Y. C. Dong and S. S. Feng, *Biomaterials*, **25**, 2843 (2004).

(49) S. Galindo-Rodriguez, E. Allemann, H. Fessi, and E. Doelker, *Pharm. Res.*, **21**, 1428 (2004).

(50) J. Cheng, B. A. Teply, I. Sherifi, J. Sung, G. Luther, F. X. Gu, E. Levy-Nissenbaum, A. F. Radovic-Moreno, R. Langer, and O. C. Farokhzad, *Biomaterials*, **28**, 869 (2007).

(51) K. L. Hoy, *The Hoy: Tables of Solubility Parameters*, Union Carbide Corporation, South Charleston, 1985.

(52) C. M. Hansen, *Hansen Solubility Parameters: A User's Handbook*, CRC Press, Boca Raton, 2000.